Supplementary Materials and Methods

Preparation of Subcellular Fraction and Protein Detection With Western Blotting

Subcellular fractions of HuS-E/2 cells and patient's tissues were prepared with the ProteoExtract Subcellular proteome Extraction Kit (Millipore, Billerica, MA) according to the manufacturer's protocol. Five micrograms of total protein of each fraction or whole-cell lysate of each cell was analyzed by Western blotting. Western blotting was performed as described previously.[1]

Collection of Total RNA and Cell Lysate From HCV-Infected Patients' Tissue

Total RNA from patients' tissue was collected with RNeasy mini (Qiagen, Hilden, Germany). In brief, frozen tissues were homogenized in lysis buffer with a Power Masher (Nippi, Tokyo, Japan). Homogenized samples were used for RNA purification according to the manufacturer's protocol. Cell lysate from tissues were collected with RIPA buffer (Thermo Scientific, Waltham, MA) or the ProteoExtract Subcellular proteome Extraction Kit according to the manufacturer's protocol.

cAMP Reporter Assay

Huh-7–derived and HuS-E/2 cells were transfected with pCRE-Luc (Agilent Technologies, Santa Clara, CA) using Fugene6 (Roche) and Effectene (Qiagen), respectively, essentially according to the manufacturers' protocols. Six hours and 2 days post-transfection of Huh-7–derived and HuS-E/2 cells, respectively, the culture medium was replaced with fresh medium containing one of the reagents. One and 3 day(s) post-transfection of Huh-7–derived and HuS-E/2 cells, respectively, luciferase activity in the cells was measured using a luciferase activity detection reagent (Promega, Madison, WI) and a Lumat LB 9507 luminometer (EG&G Berthold, Bad Wildbad, Germany).

Calcium Ion Quantification

HEK293, Huh-7–derived, and HuS-E/2 cells were treated with the calcium ionosphere A23187 (Sigma-Aldrich) and the TP agonist U-46619 for 1 day. Calcium ion concentrations were quantified using a calcium assay kit (Cayman Chemical) according to the manufacturer's protocols.

Actin Polymerization Assay

Activation of actin polymerization via TP was measured with fluorescein isothiocyanate–phalloidin (Sigma-Aldrich). After culture in lipid-free fresh medium, cells were stimulated with 10 μmol/L U46619 containing medium for 30, 60, and 180 seconds. Then, samples were stained with 10 μg/mL fluorescein isothiocyanate phalloidin, Fluorescent intensity at 520 nm was measured.

Fatty Acid Analysis

Fatty acid analysis of HCV-infected Huh-7.5 cells treated with or without Ozagrel was performed by Toray Research Center, Inc, Tokyo, Japan using gas chromatography. Total fatty acid samples were extracted from the cells according to the Bligh-Dyer[2] method.

Secondary Infection Experiments in Chimeric Mice Transplanted Human Hepatocytes

The chimeric mice were inoculated intravenously with patient serum including 1.0×10^5 genome titer of bbHCV (genotype 1b) as the first infection. Ozagrel was administered orally twice each day (300 μg/day) 1 week after the inoculation. The serum samples from those mice were collected at 5 weeks after starting the drug treatments, and used as inocula in the secondary infection experiment. Naive chimeric mice were inoculated with the collected chimeric mice serum including 1.0×10^5 genome titer of HCV. Administration of Ozagrel was started simultaneously. HCV-RNA levels in the blood of the chimeric mice at 1, 2, and 3 weeks after infection in secondary infection experiments were evaluated by qRT-PCR.

Determination of Nucleotide Sequence of HCV Genome After Treatment With Ozagrel

Chimeric mice were inoculated secondarily with sera from HCV-infected chimeric mice with or without Ozagrel treatment. Sera of these chimeric mice treated with or without Ozagrel were collected 5 weeks after the inoculation and the start of the treatment. HCV genome sequences of these samples were determined by the direct sequencing method according to the protocol described previously.[3] HCV genomic sequences obtained from sera of mice with 2 different types of treatment were compared with each other. Mice with 2 different types of treatments were as follows: first, mice inoculated secondarily with sera from the first chimeric mouse without treatment were not treated with the drug (BankIt1626925 Seq3 in GenBank). Second, mice inoculated secondarily with sera from the first chimeric mouse with treatment were treated with the drug (BankIt1626925 Seq1 in GenBank). These sequencing data were registered with GenBank (http://www.ncbi.nlm.nih.gov/genbank/).

Supplementary References

1. Kushima Y, Wakita T, Hijikata M. A disulfide-bonded dimer of the core protein of hepatitis C virus is important for virus-like particle production. J Virol 2010;84:9118–9127.
2. Bligh EG, Dyer WJ. A rapid method of total lipid extraction and purification. Can J Biochem Physiol 1959;37:911–917.
3. Kimura T, Imamura M, Hiraga N, et al. Establishment of an infectious genotype 1b hepatitis C virus clone in human hepatocyte chimeric mice. J Gen Virol 2008;89:2108–2113.

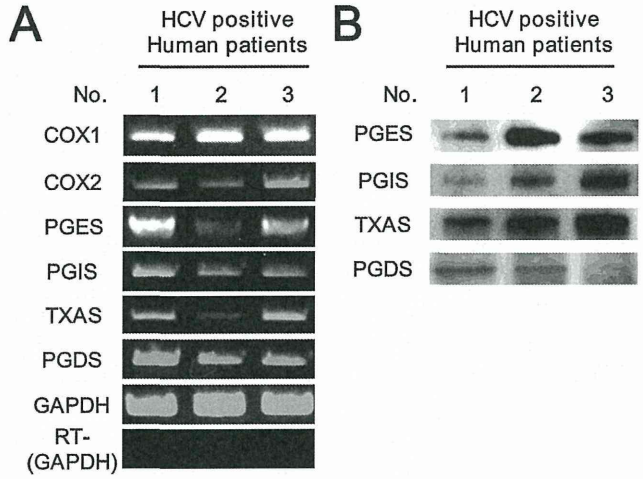

Supplementary Figure 1. Protein and mRNA levels of PG synthases in HCV-infected patient tissue. (*A* and *B*) mRNA expression and protein levels of PG synthases in HCV-infected patient tissue. Representative results from 2 independent experiments are shown.

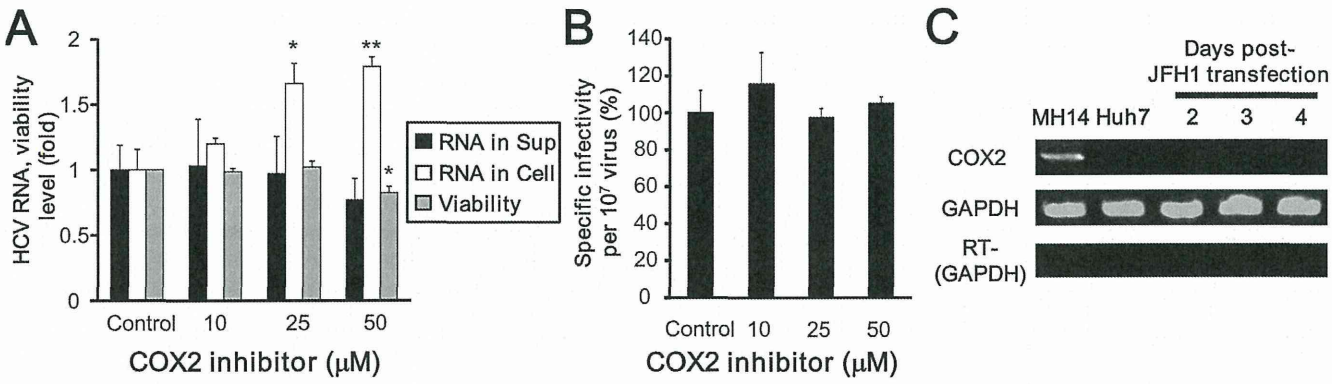

Supplementary Figure 2. Effects of COX2 inhibitor 1 on infectious HCV production. (*A*) Effects of COX2 inhibitor 1 on HCV-RNA levels in the HCVcc-producing cell-culture system. Levels of HCV RNA in medium (*black bars*) and cells (*white bars*) treated with or without COX2 inhibitor 1 were assessed with qRT-PCRs and plotted as amounts relative to results observed with control cells (control). Mean cell viability ± SD for each sample condition also is plotted (*gray bars*). (*B*) Effects of COX2 inhibitor 1 on the infectivity of HCVcc produced using the cell-culture system. (*C*) Expression of COX2 mRNA in MH14 (positive control), Huh-7, and JFH1-transfected Huh-7 cells. *Differs from control, $P < .01$; **differs from control, $P < .001$.

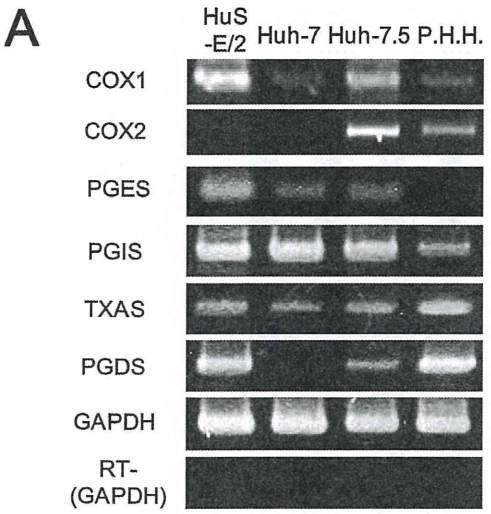

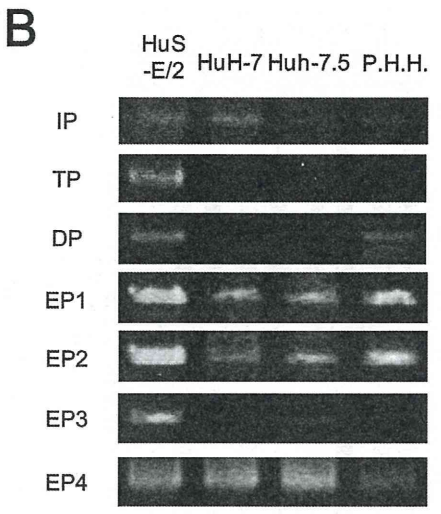

Supplementary Figure 3. Expression of PG synthase and PG-receptor mRNA in immortalized and primary hepatocyte cell lines. (*A* and *B*) mRNA expression levels of various PG synthases and PG receptors in HuS-E/2 cells, Huh-7 cells, Huh-7.5 cells, and primary human hepatocytes were analyzed in RT-PCRs. Representative results from 2 independent experiments are shown.

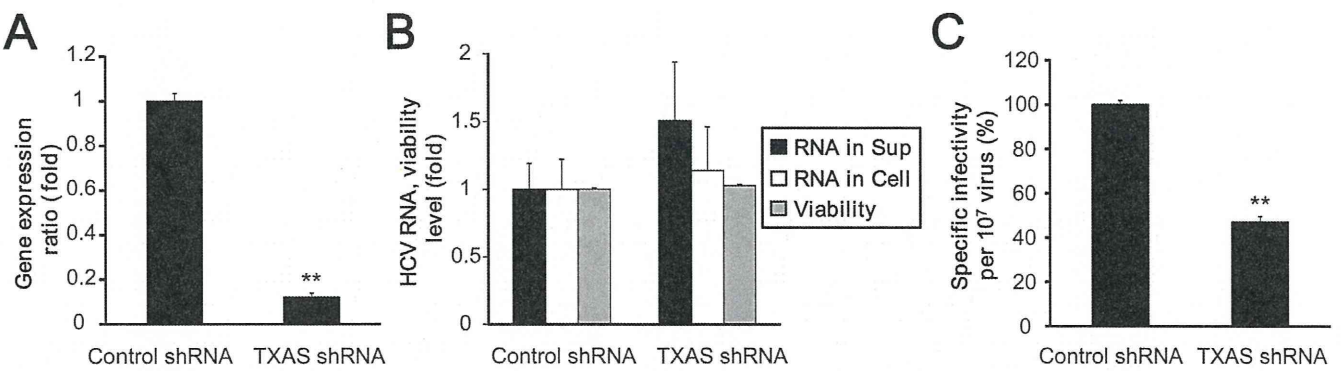

Supplementary Figure 4. Effects of short hairpin RNA (shRNA)-mediated knockdown of TXAS mRNA levels on infectious HCV production. (*A*) Knockdown of TXAS mRNA levels using shRNA. (*B*) Effects of TXAS-specific shRNA on HCV-RNA levels in the HCVcc-producing cell culture system. Levels of HCV RNA in medium (*black bars*) and cells (*white bars*) treated with control or TXAS-specific shRNA were assessed with qRT-PCRs and plotted as amounts relative to results observed with control shRNA–treated cells (control). Mean cell viability ± SD for each sample condition also is plotted (*gray bars*). (*C*) Effects of TXAS-specific shRNA on the infectivity of HCVcc produced using the cell-culture system. **Differs from control, $P < .001$.

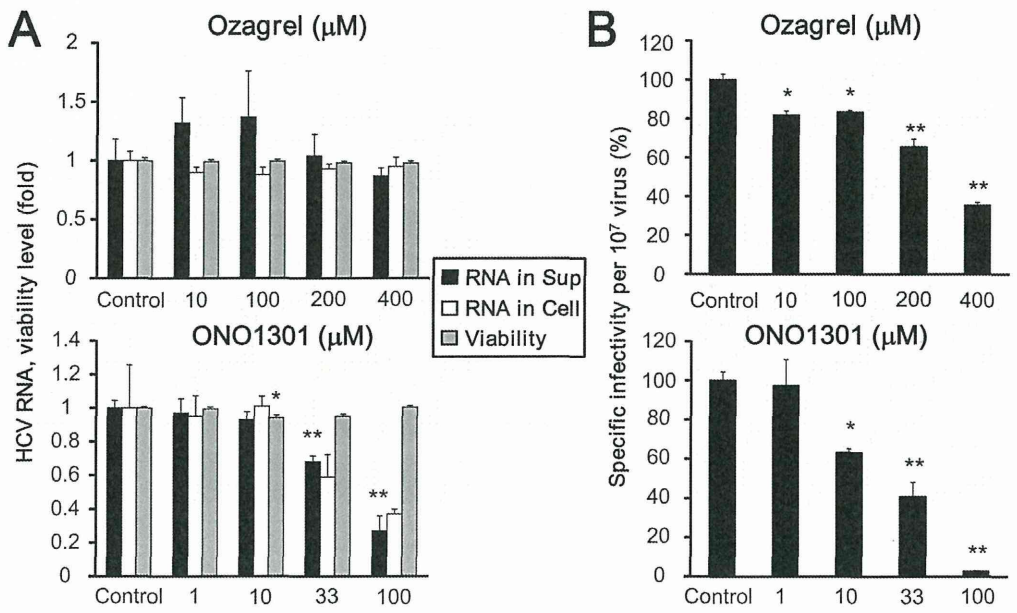

Supplementary Figure 5. Effects of Ozagrel and ONO1301 on the infectivity of HCVcc produced from J6/JFH1-transfected Huh-7.5 cells. (*A*) Effects of Ozagrel (*upper panel*) and ONO1301 (*lower panel*) on HCV-RNA levels in HCVcc-producing cell cultures. Levels of HCV RNA in the medium (*black bars*) and cells (*white bars*) treated with Ozagrel or ONO1301 cells were assessed in qRT-PCRs and plotted as the amount relative to results from untreated cells (control). Mean cell viability ± SD for each sample condition also is plotted (*gray bars*). (*B*) Effects of Ozagrel (*upper panel*) and ONO1301 (*lower panel*) on the infectivity of HCVcc produced in the cell-culture system. *Differs from control, $P < .01$; **differs from control, $P < .001$.

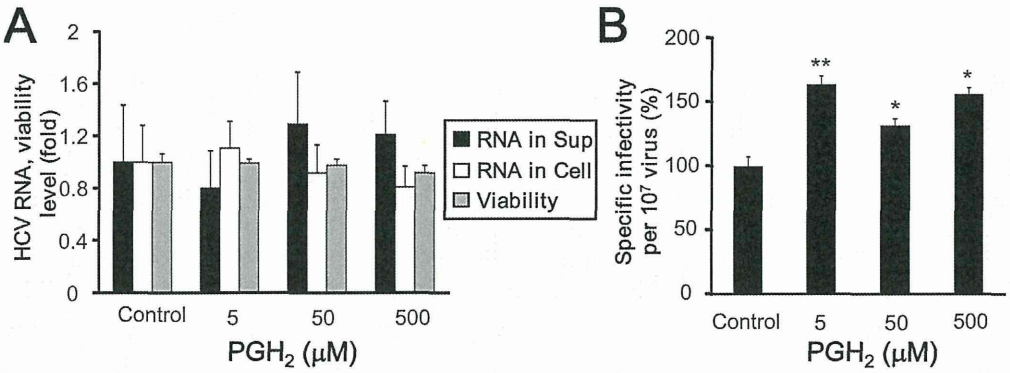

Supplementary Figure 6. Effects of PGH_2 on infectious HCV production. (*A*) Effects of PGH_2 on HCV-RNA levels in the HCVcc-producing cell-culture system. Levels of HCV RNA in medium (*black bars*) and cells (*white bars*) treated with or without PGH_2 were assessed with qRT-PCRs and plotted as amounts relative to results observed with control cells (control). Mean cell viability ± SD for each sample condition also is plotted (*gray bars*). (*B*) Effects of PGH_2 on the infectivity of HCVcc produced using the cell culture system. *Differs from control, $P < .01$; **differs from control, $P < .001$.

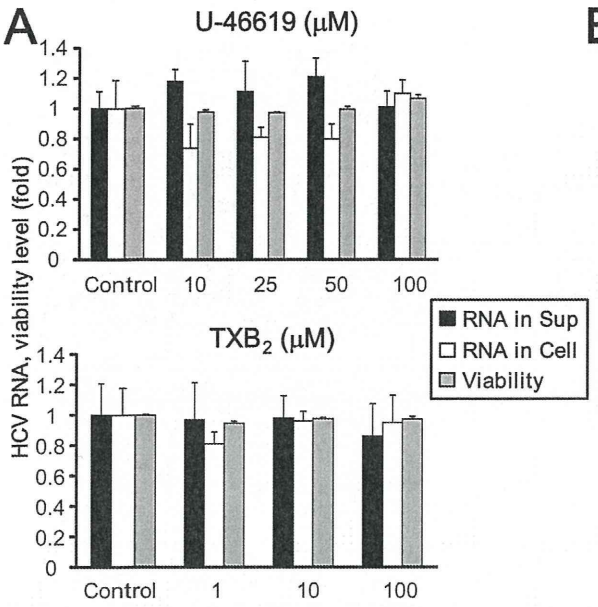

Supplementary Figure 7. Effects of U-46619 and TXB_2 on infectious HCV production. (*A*) Effects of U-46619 (*upper panel*) and TXB_2 (*lower panel*) on HCV-RNA levels in HCVcc-producing cell cultures. Levels of HCV RNA in the medium (*black bars*) and cells (*white bars*) treated with U-46619 or TXB_2 were assessed in qRT-PCRs and plotted as the amount relative to results observed with untreated cells (control). Mean cell viability ± SD for each sample condition also is plotted (*gray bars*). (*B*) Effects of U-46619 (*upper panel*) and TXB_2 (lower panel) on the infectivity of HCVcc produced in the cell-culture system were assessed.

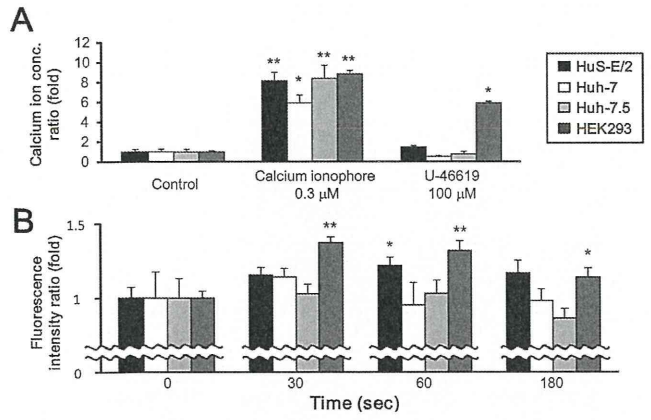

Supplementary Figure 8. Effects of U-46619 on HuS-E/2, Huh-7, Huh-7.5, and HEK293 cell lines via TP. (*A*) Concentrations of intracellular calcium ions were measured in HuS-E/2 (*black bars*), Huh-7 (*white bars*), Huh-7.5 (*gray bars*), and HEK293 (*dark gray bars*) cells treated with or without a calcium ionophore or U-46619. Calcium ion concentrations relative to those in mock-treated cells (control) were determined from triplicate wells in 2 independent experiments and are shown as means ± SD. (*B*) Actin polymerization after U-46619 treatment was measured with fluorescein isothiocyanate (FITC)-labeled phalloidin. *Differs from control, $P < .01$; **differs from control, $P < .001$.

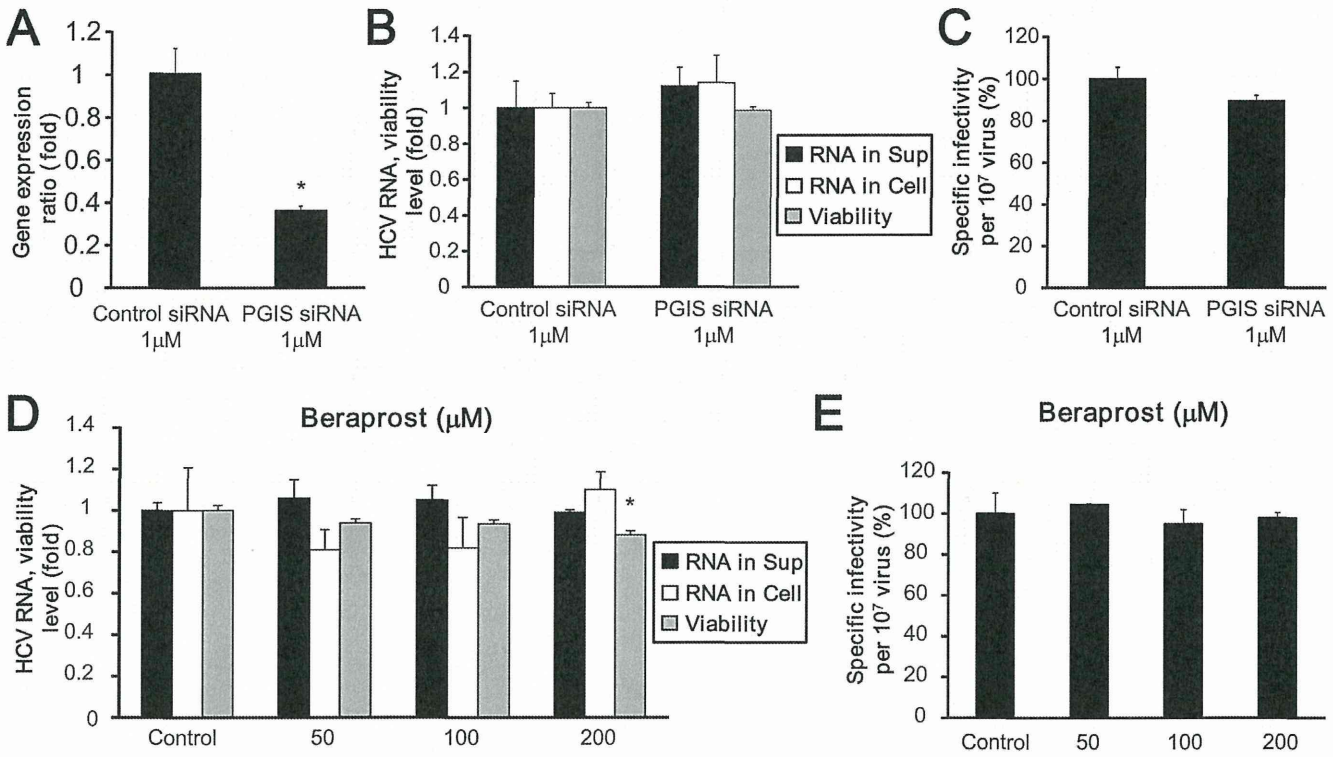

Supplementary Figure 9. Effects of PGI_2 on infectious HCV production. (*A*) siRNA-mediated knockdown of PGIS expression. (*B*) Effects of PGIS-specific siRNA on HCV-RNA levels in HCVcc-producing cell cultures. Levels of HCV RNA in medium (*black bars*) and cells (*white bars*) treated with control or PGIS-specific siRNA were assessed in qRT-PCR and are plotted as amounts relative to results obtained with control siRNA–treated cells (control). Mean cell viability ± SD for each sample condition also is plotted (*gray bars*). (*C*) Effects of PGIS-specific siRNA on the infectivity of HCVcc produced in the cell-culture system. (*D*) Effects of Beraprost on HCV-RNA levels in HCVcc-producing cell cultures. Levels of HCV RNA in medium (*black bars*) and HCVcc-producing Huh-7 cells (*white bars*) treated with Beraprost were assessed in qRT-PCRs and plotted as amounts relative to results obtained with untreated cells (control). Mean cell viability ± SD for each sample condition also is plotted (*gray bars*). (*E*) Effects of Beraprost on the infectivity of HCVcc in culture medium from HCVcc-producing cell cultures were assessed. *Differs from control, $P < .01$.

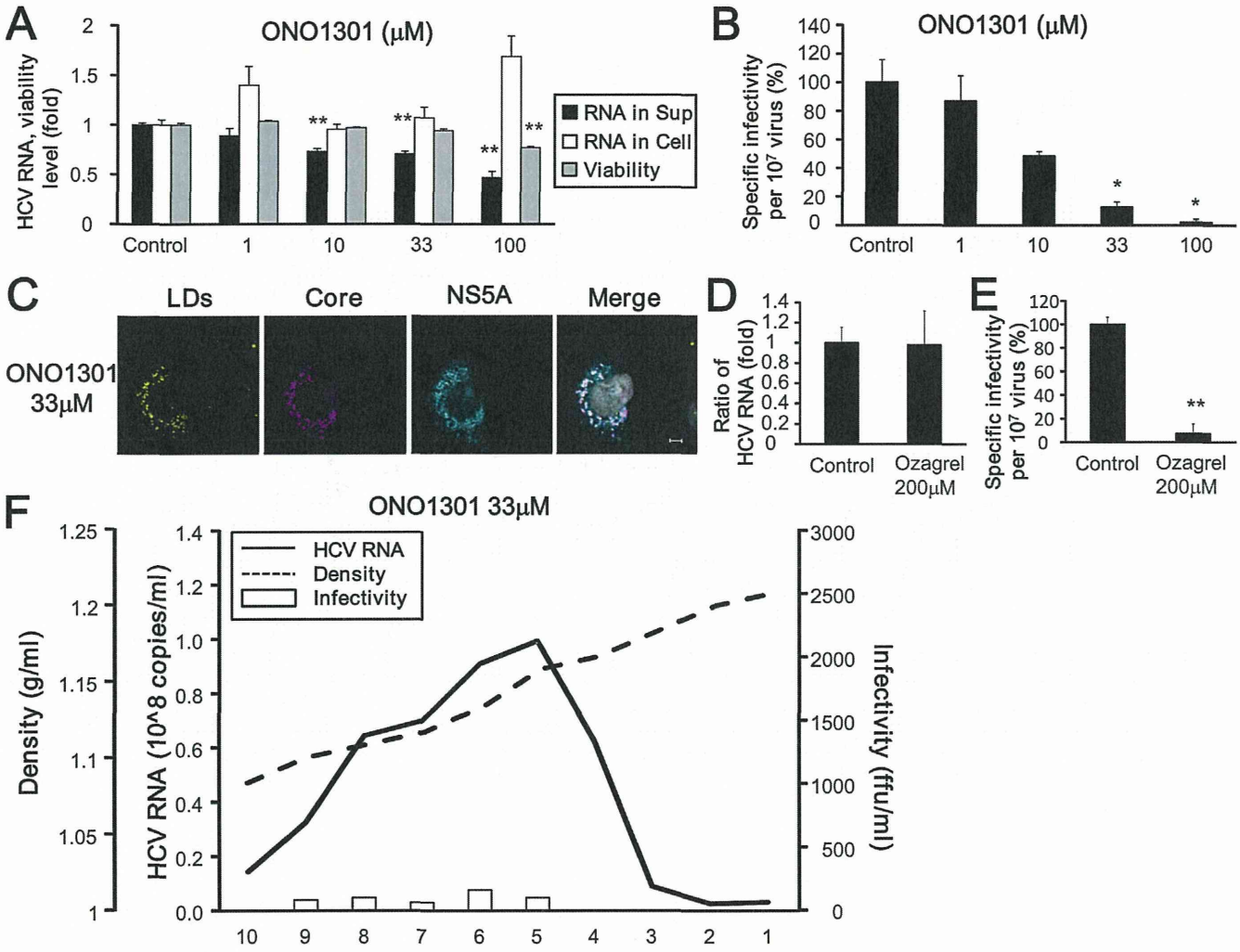

Supplementary Figure 10. Effects of ONO1301 on HCV lifecycle. (*A*) Levels of HCV RNA in medium (*black bars*) and cells (*white bars*) treated with or without ONO1301 were assessed. Mean cell viability ± SD for each sample condition also is plotted (*gray bars*). (*B*) The infectivity of HCVcc in culture medium from HCVcc-producing cell cultures treated with or without ONO1301 was assessed. (*C*) Subcellular locations of HCV core and NS5A proteins around LDs in the presence of ONO1301. Scale bars, 5 μm. (*D* and *E*) Levels and infectivity of intracellular HCV obtained from the cells treated with ONO1301. (*F*) Buoyant density of HCVcc obtained using cells treated with ONO1301. HCV RNA (*solid line*), fraction density (*dotted line*), and HCV infectivity (*white bars*) in each fraction collected by ultracentrifugation. *Differs from control, $P < .01$; **differs from control, $P < .001$.

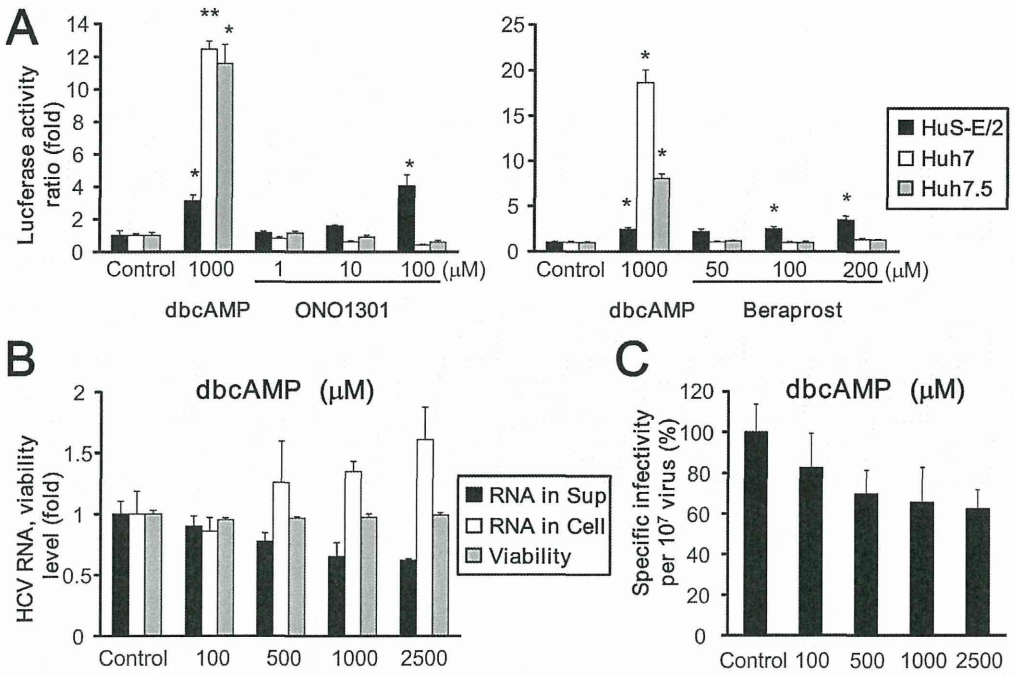

Supplementary Figure 11. Effects of dibutyryl cAMP (dbcAMP) on cell cultures producing JFH1 HCVcc. (*A*) HuS-E/2 (*black bars*), Huh-7 (*white bars*), and Huh-7.5 (*gray bars*) cells were transfected with CRE-Luc plasmid. Then, the luciferase activity in each sample was measured. Values were obtained from quadruplicate wells in 2 independent experiments and are shown as means ± SD. (*B*) Effects of dbcAMP on HCV-RNA levels in HCVcc-producing cell cultures. Levels of HCV RNA in medium (*black bars*) and cells treated with dbcAMP (*white bars*) were assessed in qRT-PCRs and plotted as amounts relative to results obtained with mock-treated cells (control). Mean cell viability ± SD for each sample condition also is plotted (*gray bars*). (*C*) Effects of dbcAMP on the infectivity of HCVcc produced using the cell-culture system. *Differs from control, $P < .01$; **differs from control, $P < .001$.

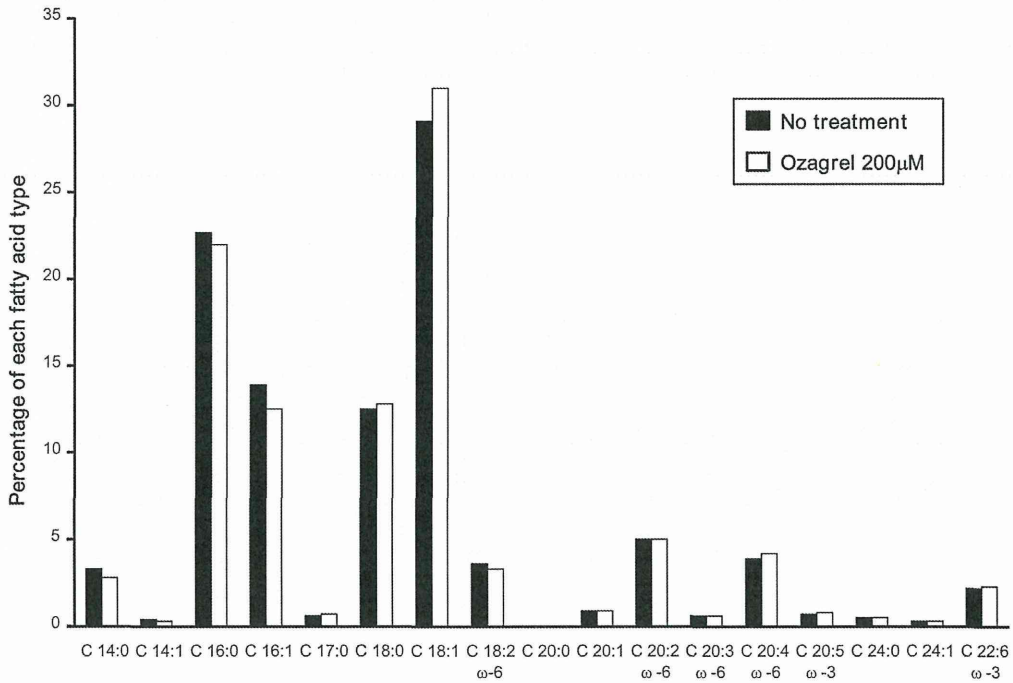

Supplementary Figure 12. Comparison of composition of fatty acids in HCV-infected Huh-7.5 cells with or without Ozagrel treatment.

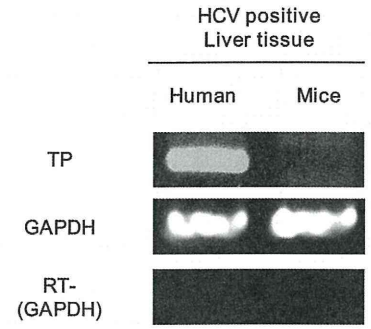

Supplementary Figure 13. Expression of TP mRNA in liver tissues from human patients and chimeric mice infected with HCV.

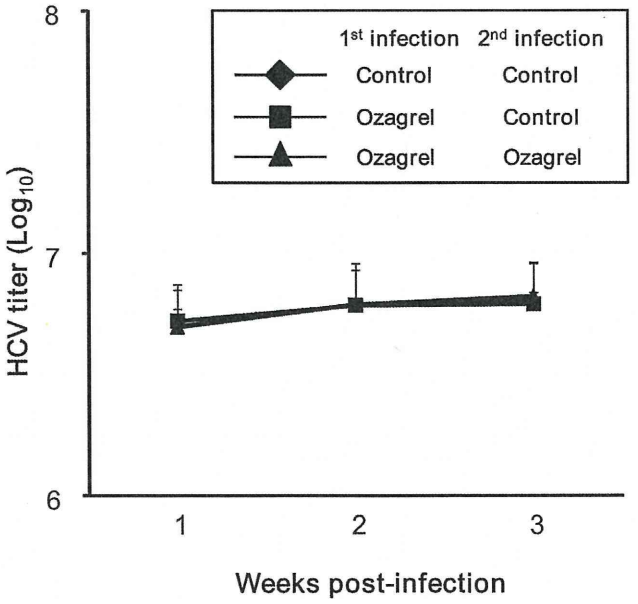

Supplementary Figure 14. Secondary infection of HCV derived from the chimeric mice model. Data are presented as means ± SD for 4 samples.

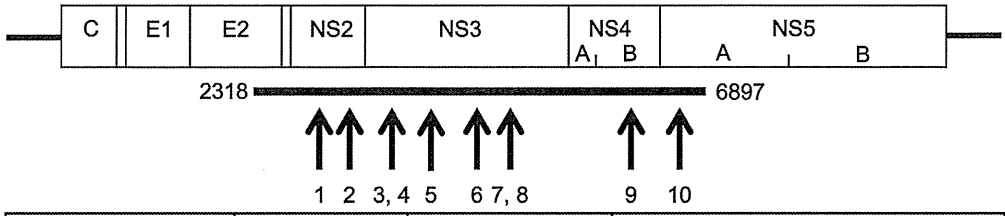

Supplementary Figure 15. Base substitutions in HCV genome collected from mice serum during a secondary infection. HCV genomic sequences from mice sera with Ozagrel treatment during primary and secondary infection was compared with those from mice without any treatment during both infection experiments. The region of obtained HCV genomic sequences is indicated (*thick bar*). The nucleotide positions of each base substitution are shown (*arrows*). Positions of base substitutions, and types of base substitution and amino acid replacement are listed in the *lower panel*.

Number of substitution point	Position of nucleotide	Single base substitution	Amino acid replacement
1	3192	A→G	Asparagine→Aspartic acid
2	3264	A→G	Isoleucine→Valine
3 4	3596 3597	T→A C→T	Phenylalanine→Tyrosine
5	3859	C→T	Serine→Leucine
6	4283	G→A	Methionine→Isoleucine
7 8	4437 4439	G→A T→C	Glycine→Serine
9	5886	G→A	Valine→Methionine
10	6747	G→A	Alanine→Threonine